Environmental Science and Pollution Research (2021) 28:14694–14706
https://doi.org/10.1007/s11356-020-11679-y

RESEARCH ARTICLE

Continuous adsorptive removal of glimepiride using multi-walled carbon nanotubes in fixed-bed column

Ismail Badran[1] · Obada Qut[2] · Abdallah D. Manasrah[3,4] · Murad Abualhasan[5]

Received: 18 August 2020 / Accepted: 15 November 2020 / Published online: 20 November 2020

Abstract

Water pollution by emerging pollutants such as pharmaceutical and personal care products is one of today's biggest challenges. The presence of these emerging contaminants in water has raised increasing concern due to their frequent appearance and persistence in the aquatic ecosystem and threat to health and safety. The antidiabetic drug glimepiride, GPD, is among these compounds, and it possesses adverse effects on human health if not carefully administered. Several conventional processes were proposed for the elimination of these persistent contaminants, and adsorption is among them. Therefore, in this study, the adsorptive removal of GPD from water using multi-walled carbon nanotubes (MWCNT) supported on silica was explored on a fixed-bed column. The effects of bed-height, solution pH, and flow rate on the adsorptive removal of GPD were investigated. The obtained adsorption parameters using Sips, Langmuir, and Freundlich models were used to investigate the continuous adsorption. The results showed that the drug removal is improved with the increasing bed height; however, it decreased with the flow rate. The effect of pH indicated that the adsorption is significantly affected and increased in acidic medium. The convection-dispersion model coupled with Freundlich isotherm was developed and used to describe the adsorption breakthrough curves. The maximum adsorption capacity (q_m) was 275.3 mg/g, and the axial dispersion coefficients were ranged between 3.5 and 9.0 × 10^5 m^2/s. The spent adsorbent was successfully regenerated at high pH by flushing with NaOH.

Keywords Glimepiride · Continuous adsorption · Convection–dispersion model · Multi-walled CNT · Wastewater

Introduction

Pharmaceuticals and personal care products (PPCP) are often considered one of the contemporary emerging pollutants. Such man-made products are now present in water resources across the globe (Badran et al. 2020; Badran and Talie 2020; Bradley et al. 2016; Kibuye et al. 2019; Kot-Wasik et al. 2016; Li et al. 2016; Luo et al. 2014; Markiewicz et al. 2017). These

Responsible Editor: Ester Heath

Highlights
- Rapid and efficient removal of the antidiabetic drug glimepiride by MWCNT
- The continuous adsorption breakthrough curve is described by a new convection–dispersion model.
- The adsorption efficiency increases as the solution becomes more acidic, in agreement with the ZPC of the MWCNT, and the pK_a of the drug.
- The column bed was successfully regenerated through flushing with dilute NaOH.

✉ Ismail Badran
ibadran@qu.edu.qa

[1] Department of Chemistry and Earth Sciences, Qatar University, P.O. Box: 2713, Doha, Qatar

[2] Department of Chemistry, An-Najah National University, P.O. Box 7, Nablus, Palestine

[3] Department of Chemical and Petroleum Engineering, University of Calgary, 2500 University Street NW, Calgary, Alberta T2N 1N4, Canada

[4] Carbon OxyTech Inc., 3655 36 Street NW, Calgary, Alberta T2L 1Y8, Canada

[5] Department of Pharmacy, An-Najah National University, P.O. Box 7, Nablus, Palestine

compounds find their ways into water systems through different pathways such as human and animal excretion, careless disposal, and soil drainage (Couto et al. 2019; Kot-Wasik et al. 2016). Wastewater treatment plants (WWTP) are actually considered the primary source of PPCP pollution, owing to their outdated designs (Gadipelly et al. 2014; Kot-Wasik et al. 2016). The presence of PPCP in water resources may pose hazards to human and non-target organisms (Carrales-Alvarado et al. 2020; Fent et al. 2006; Gadipelly et al. 2014; Kibuye et al. 2019; Kot-Wasik et al. 2016; Luo et al. 2014). Antibiotic resistance, infertility, endocrine disruption, and allergy are just a few examples of modern diseases that are partially caused by PPCP pollution (Alnajjar et al. 2019; Mackul'ak et al. 2019; Niemuth et al. 2015; Zhu et al. 2017). In addition, the by-products of PPCP biotransformation can be very harmful (Mackul'ak et al. 2019).

The reliance on soil to act as a good filter for water pollutants is uncertain (Biel-Maeso et al. 2018). In their assessment of WWTP performance, researchers recently reported that PPCP can still present up to 14 months in plants and irrigating groundwater in WWTP surrounding areas. The investigated PPCPs, including naproxen, sulfamethoxazole, trimethoprim, and ofloxacin, were considered to pose medium to high risk to aquatic organisms (Kibuye et al. 2019).

Adsorptive removal is an effective technique to treat wastewater from PPCP (Ahsan et al. 2020; Alnajjar et al. 2019; Badran et al. 2019a; Badran and Khalaf 2019; Badran et al. 2019b; Gadipelly et al. 2014; Jasim et al. 2013; Sarkar et al. 2014; Sylvia et al. 2018). Complete removal can then be achieved through advanced oxidation or photodegradation (Ajmal et al. 2014; Badran et al. 2019a; Badran et al. 2020; Badran et al. 2019b; Dong et al. 2015; Manasrah and Nassar 2020; Sarkar et al. 2014). Despite the extensive research on PPCP removal by adsorption, most studies are conducted in batch mode that is not easily scalable (Gadipelly et al. 2014; Jasim et al. 2013; Li et al. 2019). Thus, this work aims to provide a proof-of-concept for a rapid, efficient, and continuous-flow technique for PPCP adsorption.

Among several types of nanomaterials, carbon nanotubes (CNT) have emerged as successful candidates for many applications, including their use as efficient adsorbents. CNT possess high surface area and superior electronic, magnetic, and thermal properties (Carrales-Alvarado et al. 2020; El-sayed 2020; Manasrah et al. 2016; Manasrah et al. 2018). They can be also engineered to serve different functions and are highly mobile in porous media (Altowayti et al. 2019; Liu et al. 2009). Some argue that the high cost of CNT would limit their industrial implementation. However, the cost is projected to decline under the high demand and the variety of production methods. It is estimated that the CNT market is valued at $1033 million and is expected to reach $3812 million by 2022 (Allied Market Research 2020).

The antidiabetic drug glimepiride (Scheme 1) was chosen for this study as a potential wastewater pollutant. Glimepiride (GPD) is a second-generation high potency sulfonylurea hypoglycemic (antidiabetic) drug. These agents have sulfonamide structural analogues that do not possess antibacterial activity (Gangji et al. 2007). These drugs target a specific receptor in the β cells of islets of Langerhans, called sulfonylurea receptors, and cause depolarization by reducing the conductance of ATP-sensitive potassium channels. This enhances the Ca^{2+} influx and produces degranulation, leading to the secretion of insulin (Gribble and Reimann 2003; Proks et al. 2002). The complex aromatic structure of these compounds compared with the first-generation sulfonylurea hypoglycemic drugs facilitates receptor binding and makes it extensively bound to plasma proteins thus prolonging its duration of action (Abraham et al. 2010). Sulfonylurea drugs are metabolized by liver cytochrome enzymes primarily by oxidation of the cyclohexyl mainly by CYP2C9 enzyme (Marchetti and Navalesi 1989).

GPD was approved by the FDA in the USA in 1995 for the treatment of type-II diabetes mellitus. The most dangerous adverse reaction resulting from sulfonylureas is causing severe hypoglycemia (low blood sugar) (Jasim et al. 2013; Kiran et al. 2009). Elderly people and patients with reduced renal functions have a higher risk of getting hypoglycemia when administering sulfonylureas (Saudek et al. 2006). Hematological complications (e.g., thrombocytopenia), cholestatic hepatitis, and general allergic reactions were also reported. Frequently reported side effects include nausea, heartburn, weight gain, bloating, skin rashes, and weight gain. The FDA warns that sulfonylureas could increase cardiovascular risks due to the mild diuretic effect, enuresis it induces when taken for a long time (Asplund et al. 1983; Burge et al. 1998).

To the best of our knowledge, few studies have been reported on the adsorptive removal of GPD. A group of researchers have studied the in-soil adsorption of GPD, among other pharmaceuticals, and determined to biodegrade slowly with half-life values between 20 and 40 days, signaling a potential threat to ground and surface water (Mrozik and Stefańska 2014). Jasim *et al.* have studied the batch adsorption of GPD using activated charcoal and Iraqi kaolin in aqueous media (Jasim et al. 2013). The adsorption followed Freundlich isotherm and was highly pH dependent. Their results also showed that the adsorption performed using charcoal is better than the kaolin and favored lower temperatures (Jasim et al. 2013).

In this study, a lab-scale setup that consists of a fixed-bed adsorber was constructed for the continuous-flow adsorption of GPD. Multi-walled carbon nanotubes (MWCNT) dispersed in silica were used as an adsorbent. The effects of bed height, the solution flow, the pH, and the amount of adsorbent were studied. The breakthrough curve describing the adsorption behaviors was analyzed using a developed convection-dispersion model coupled with Freundlich isotherm and compared with commercial adsorption models such as Adams–

Scheme 1 Molecular structure of glimepiride

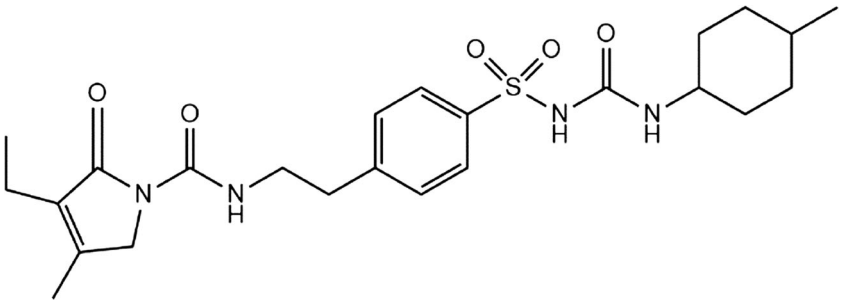

Bohart and Thomas. The study also attempted to regenerate the adsorbent by using deionized water or dilute NaOH.

Experimental work

Materials and methods

Glimepiride (99.0%, M.Wt. 490.62 g/mol) was obtained from Alfa Aesar (Tewksbury, MA, USA). Commercial multi-walled carbon nanotubes (MWCNTs, 95%) were purchased from Chengdu Organic Chemicals Co. Ltd. (Chengdu, Sichuan, China). Acetonitrile (99.8 %), white silica (mesoporous, 99.9%), and other reagents used to prepare the buffers including borax, NaOH, HCl, KH_2PO_4, KHP, and acetic acid were of high purities and were obtained from Sigma-Aldrich Chemical Company (Milwaukee, Wisconsin, USA). The scanning electron microscope (SEM) images for MWCNT before and after the GPD adsorption were collected using a field emission instrument (Nova Nano SEM 450) operating at 5 kV and equipped with an energy-dispersive X-ray analyzer (EDX, Bruker). The pH of the solutions was measured using a Jenway 3510 pH meter (Jenway, Staffordshire, UK). A Lab Tech shaker (Daihan Labtech, Korea) was used to sonicate the samples as required. A UV–Vis spectrophotometer (UV-1800, Shimadzu, Canby, OR, USA) coupled to a temperature controller (Fried electric device WBH-060N) was used to obtain the spectra of the drug and follow the adsorption process. Sample weighing was done using an analytical balance (ASB-310-C2-V2, MRC Lab Equipment. Essex, UK). The peristaltic pump (model PP-F-380, with head model LEAD-15-44, Longer Precision Pump Co., Ltd, Baoding, Hebei, China) that is used in this work is an 8-channel, 4 rollers with a flow rate between 1 and 380 mL/min. The pump was supplied by Biotech Medical Supplies, Ramallah, Palestine.

Solution preparation

A stock solution of glimepiride (GPD) was prepared by dissolving 25.0 mg of GPD powder in 1.0 L of 50:50 acetonitrile/deionized water mixture. The bottle was sealed and covered with aluminum foil for no longer than 3 days. Standard solution of GPD of different concentrations was prepared by diluting the previously prepared stock solution as needed. The buffers used to control the pH of solutions were prepared as explained in our previous work (Badran and Khalaf 2019). Further details on the validation of the analytical method including the sensitivity, selectivity, and detraction limits are provided in the supplementary information section.

The experimental setup

The experimental setup is constructed by connecting the container of the GPD stock solution to a 20-cm quartz adsorption bed through a peristaltic pump. The bed has a cross-sectional area of 1.0 cm^2. All connections were made of 1.34-mm-ID Teflon tubing. The bed column was filled by a mixture of MWCNT supported on white silica. The MWCNT were dispersed manually, in definite ratios, with the silica at ambient conditions. Silica was used as a support because it is a standard industrial material used in wastewater filtration as well as for its availability and low cost. Two sheets of glass wool were placed below and on top of the MWCNT/silica layer to prevent MWCNT from flowing into the effluent. Samples were withdrawn from the adsorption column into a collection container to be analyzed by UV–Vis spectrophotometry.

Adsorption experiments

The batch experiments were performed by pipetting 10 mL of the standard 25-mg/L solutions to 30.0-mL small plastic vials, followed by addition of different masses of MWCNT in the range of 2–100 mg. The solutions were shaken for 30 min at room temperature and then allowed to settle for 4 h. Samples from the aliquots were taken for UV–Vis measurements without any filtration to avoid disturbing the concentration of GPD.

The continuous adsorption experiments were conducted in the fixed-bed column after filling the adsorption bed with a known mixture of MWCNT/silica composite. Then, the peristaltic pump was connected between the sample container and the adsorption column. The system was checked for any leaks before it was flushed with deionized water for 10 min. Then, the liquid solution is pumped from the sample container into the adsorption column at a constant flow rate, pre-estimated. The effluent samples were then collected periodically in small

vials for immediate UV–Vis analysis. The glass tube was cleaned and refilled with a fresh batch of adsorbent before the next run.

Modeling of continuous adsorption Adsorption in a fixed-bed adsorber is a time- and distance-dependent phenomenon (Worch 2012). The process is typically described by a breakthrough curve (BTC) as illustrated in Fig. 1. The adsorption starts by injecting a sample of known concentration, C_0, through the adsorption column (bed), which is filled with an adsorbent. The performance of the fixed-bed system was evaluated at room temperature by measuring the effluent concentration at the outlet of the column at different time intervals by UV–Vis absorption spectroscopy using a measured extinction coefficient from Beer's law analysis. As shown in the figure, the measured initial concentration of GPD at the outlet is almost zero. The change in the outlet concentration of GPD, C, over time is recorded at the outlet of the column. Then, the BTC can be constructed by plotting the ratio C/C_0 vs. time interval (Ghosh et al. 2015; Hethnawi et al. 2020a; Worch 2012).

Initially, the adsorption is usually rapid with a significant drop in the sample concentration. As time goes, the adsorption becomes weaker due to gradual coverage of the adsorbent sites. The sudden increase in the ordinate value represents the break point (T_b). Implicitly, a late T_b is favored for higher adsorption capacities. In the fixed-bed column, the adsorption equilibration takes place within part of the column, known as the mass-transfer zone (MTZ) or adsorption zone. As time goes, the zone moves across the column until an exhaustion point is reached, as illustrated in Fig. 1 (Hethnawi et al. 2020a; Hethnawi et al. 2017a; Tian et al. 2013).

Several simple mathematical models were established to describe the dynamic behavior of the BTC. Thomas model, for instance, assumes plug flow behavior in the bed and uses Langmuir isotherm for equilibrium, and second-order reversible reaction kinetics. (Thomas 1944). It is suitable for adsorption process where the external and internal diffusion limitations are extremely small, as per the equation

$$\frac{C}{C_0} = \frac{1}{1 + e^{\left(k_{TH} q_0 \frac{x}{v} - k_{TH} c_0 t\right)}} \tag{1}$$

where C is the adsorbate concentration (mg L^{-1}) at time t (min), C_0 is the initial concentration, k_{TH} is the Thomas rate constant (mL mg^{-1} min^{-1}), q_0 is the total adsorption capacity (mg g^{-1}), v is the flow rate (mL/min), and x is the packed mass (g) of the material in the fixed bed. Thus, by plotting the left term ($\frac{C}{C_0}$) with time, a nonlinear curve fitting can be applied according to Eq. 1 to produce the unknown parameters, k_{TH}, q_0. Such fitting was performed in OriginLab (OriginLab Corporation 2020) according to the following mathematical equation:

$$y = \frac{1}{1 + e^{(ab - cx)}} \tag{2}$$

By implementing the sigmoidal function of Eq. 2, one can obtain the ideal break point time (cf. Fig. 2) as it is equal the ratio of ab/c.

Similarly, a widely used model was proposed by Adams and Bohart (Bohart and Adams 1920). The main assumption of the model is based on the proportionality between the rate of adsorption and both the residual adsorbent and adsorbate concentration. The model was originally proposed for gas-solid adsorption, but it has been extended to other systems according to the equation

$$\frac{C}{C_0} = \exp\left(k_{AB} C_0 t - k_{AB} N_{AB} \frac{Z}{F}\right) \tag{3}$$

where C and C_0 are defined as above. k_{AB} is the Adams-Bohart rate constant (mL mg^{-1} min^{-1}), and N_{AB} is the saturation concentration (mg L^{-1}). F is the cross-sectional flow rate (cm min^{-1}) and Z of the bed height (cm). Using nonlinear curve fitting, the unknown parameters N_{AB} and k_{AB} can be

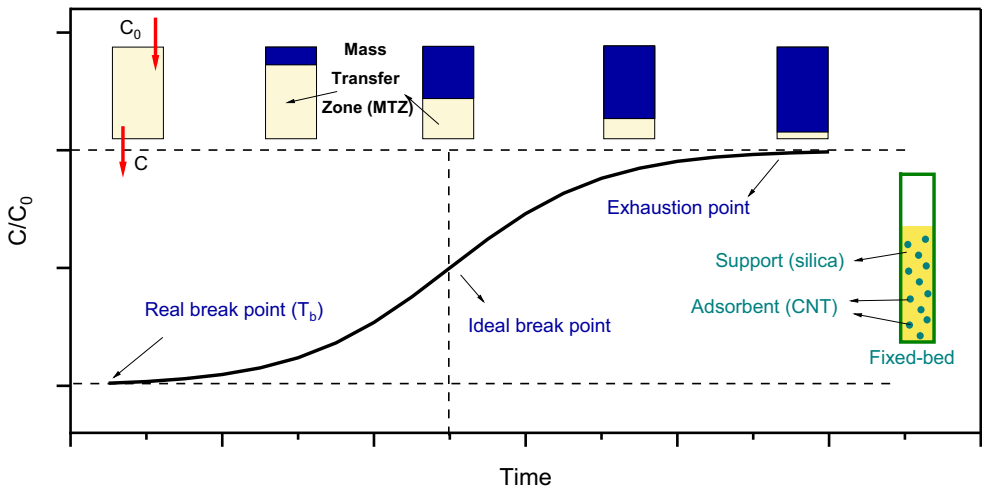

Fig. 1 Schematic representation of an ideal breakthrough curve, and the movement of the mass-transfer zone (MTZ) through time

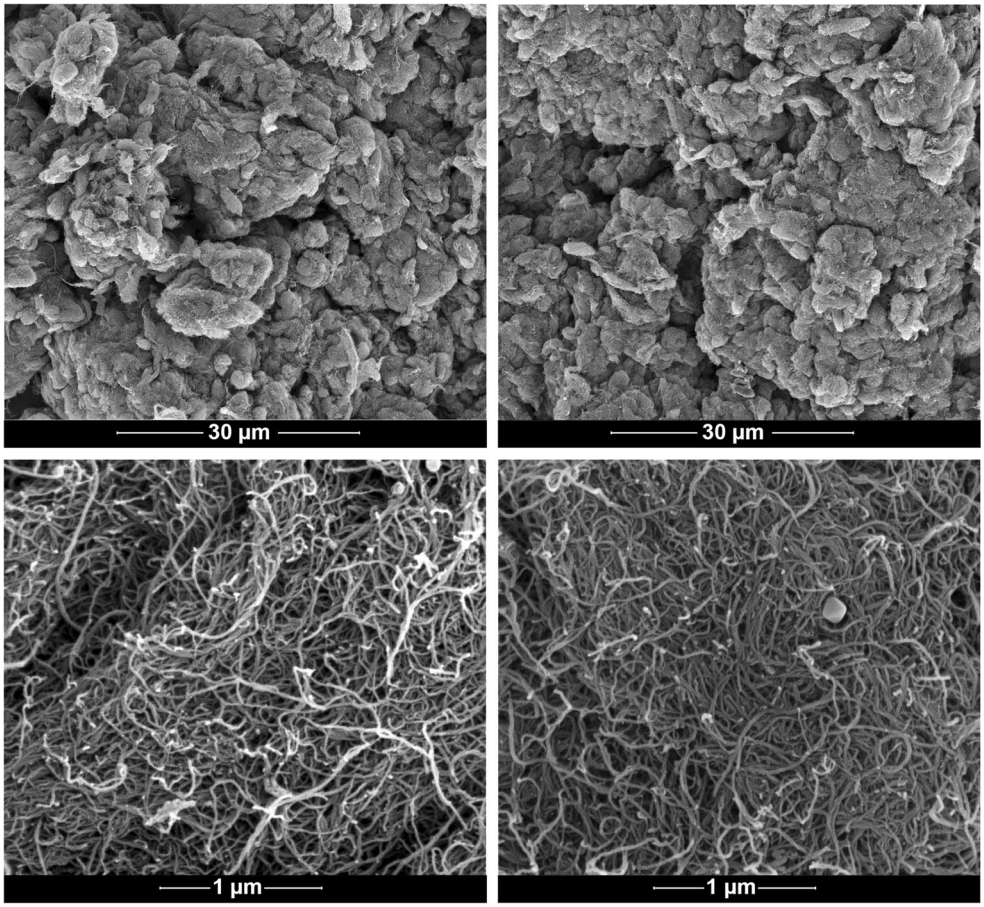

Fig. 2 Scanning electron microscope (SEM) images with different magnifications for the MWCNT before adsorption (left) and after adsorption (right) using 25 mg/L GPD solution

determined.

Nevertheless, it is too difficult to describe the dynamic behavior of a compound in a fixed bed under defined operating conditions, as the process does not occur at a steady state while the influent still passes through the bed. The dynamic adsorption model usually consists of a macroscopic mass conservation equation, uptake rate equation, and isotherm. Therefore, models derived from different assumptions, such as Adams-Bohart and Thomas, are only suitable for a limited situation in possibly predicting the dynamic behavior of the bed in column performance. However, they fail to describe others (Xu et al. 2013). For instance, the Thomas model neglects the axial dispersion in the adsorption column, and thus cannot describe the adsorption behavior under plug flow. Similarly, the Adams–Bohart model is used for the description of the initial part of the breakthrough curve, and thus, it is limited to the range of the condition used (Sylvia et al. 2018).

Therefore, a theoretical model for determining the dynamic adsorption and diffusion of the pollutant in the fixed bed under the influence of different operational parameters is needed. The adsorption process takes place when the wastewater stream enters the fixed-bed column. As time passes, adsorption starts, and the initial GPD concentration at the outlet is almost zero until the breakpoint, where the GPD concentration starts to increase until it reaches saturation point. A mathematical convection-dispersion model describing the dynamic behavior of the adsorption process through fixed-bed column has been recently developed (Hethnawi et al. 2020a; Hethnawi et al. 2017a; Hethnawi et al. 2017b). The model assumed that there is no radial diffusion (traverse diffusion) along the column due to its considerable length. The significance of this proposed model is not only the prediction of the breakthrough curves but also the sensitivity and the steepness of BTC due to the adsorption term as a function of time which can be represented by any reported isotherm model like Sips, Langmuir, and Freundlich models. In the convection-dispersion model, the mass balance of the adsorbed compound is described by a set of convection-diffusion equations coupled with source terms related to the adsorption and diffusion inside the porous adsorbent particles, as per the following second-order partial differential equation:

$$-D_L\frac{\partial^2 C}{\partial ‡^2}+v\frac{\partial C}{\partial ‡}+\frac{\partial C}{\partial t}+\frac{1-\epsilon}{\epsilon}\left(\frac{\partial q}{\partial t}\right)=0 \tag{4}$$

where D_L is the axial dispersion coefficient (m/s^2), C is the bulk adsorbate concentration in the fluid running through the bed (mg/L), ‡ is the distance (m), t is the time (min), v is the

interstitial velocity (m/s), ϵ is the porosity (unitless), and $\left(\frac{\partial q}{\partial t}\right)$ represents the variation of adsorption amount which can be described by the Freundlich model in this study. In this case, the derived form of the Freundlich model can be described by the following equation:

$$\frac{\partial q_e}{\partial t} = \frac{1}{n} K_f C^{\frac{1}{n}} \frac{\partial C}{\partial t} \tag{5}$$

By combining Eq. (4) and Eq. (5), the convection–dispersion model presents as the following:

$$-D_L \frac{\partial^2 C}{\partial ‡^2} + v\frac{\partial C}{\partial ‡} + \frac{\partial C}{\partial t} + \frac{1-\epsilon}{\epsilon}\left(\frac{1}{n} K_f C^{\frac{1}{n}} \frac{\partial C}{\partial t}\right) = 0 \tag{6}$$

The following equations represent the initial and boundary conditions:

$$C\,(‡, 0) = 0 \;\; (0 < ‡ < L) \tag{7}$$

$$‡ = 0, \;\; C_{in} = C - \left(\frac{D_L}{v}\right)\left(\frac{\partial C}{\partial ‡}\right) \; (0 < t < \infty) \tag{8}$$

$$‡ = \mathrm{L}, \frac{\partial C}{\partial ‡} = 0 \;\; (0 < t < \infty) \tag{9}$$

The non-linear partial differential equation, Eq. (6), was solved numerically together with the initial and boundary conditions (Eqs. 7–9) using NDSolve code along with the method-of-lines technique by Mathematica (v.12.0.0). Then, a mathematical algorithm was developed to fit the experimental data with the numerical solution using a manipulating code to evaluate the effective diffusivity (D_L) and the fitting parameter by minimizing the square root of the sum of the squares of residuals between the numerical values and experimental data. More details about the numerical solutions for the proposed model can be found in previous studies (Hethnawi et al. 2020a; Hethnawi et al. 2017a; Hethnawi et al. 2017b). By applying these models, the breakthrough curves are expressed in terms of normalized concentration, $\left(\frac{C}{C_0}\right)$, as a function of time.

Results and discussion

Batch experiments

Adsorption isotherms

Figure S1 (supplementary information section) shows the room-temperature UV–Vis spectrum of the stock solution of GPD (25 mg/L). Visually, the GPD solution was colorless, which is reflected by the absence of any absorption peaks in the visible region. However, the drug absorbs strongly in the UV region with a maximum wavelength (λ_{max}) at 229 nm. This allowed the determination of the GPD concentration in the samples according to Lambert-Beer's law. A calibration curve was constructed by preparing standard solutions of GPD using a 1:1 ratio of acetonitrile/water mixture in the range of 2–25 mg/L. A typical calibration curve is shown in Fig. S2. The error bars in the figure represent the standard deviation among three trials. A good linear regression was obtained with an R^2 of 0.9987. Thus, the concentration of GPD in the effluent samples was obtained by plugging their absorbance into the linear regression equation of the calibration curve. The detection limit of the method was determined to be 0.69 mg/L. The sensitivity of the method was determined from the slope of the calibration curve, and it is equal to 0.05 mg^{-1} L. Further details on the method validation are provided in the supplementary information section.

Scanning electron microscope (SEM) images were taken for the MWCNT samples before and after the batch adsorption experiments as shown in Fig. 2. According to the SEM analysis, the MWCNT used in this work were 100 nm to a few micrometers in length and ~ 15 nm in width. The images show no significant changes in the MWCNT morphology after adsorption. MWCNT are known to have a dual functionality on both their surface and inside the tubes (Charumathi and Das 2012; Manasrah et al. 2016; Tian et al. 2013). This, along with the low concentration of the drug, 25 mg/L, can explain the absence of any visual differences in the SEM images. Nevertheless, the EDX analysis (cf. Figs. S6–S8) shows a notable increase in the O, S, and N signals after adsorption, indicating that GPD was indeed adsorbed into the MWCNT. The percentages of elemental C, N, O, and S are tabulated in Table 1. The EDX analysis for pure MWCNT, before adsorption, shows mainly signals for C (~ 97%) with little O (~ 3%). After adsorption, the carbon content decreased to *ca.* 83%, with an increase of N, O, and S to *ca.* 9, 6, and 1%, respectively. The EDX analysis for pure GPD is also shown for comparison.

As mentioned earlier, batch adsorption experiments were performed using GPD in order to reveal its adsorption behavior and to use the adsorption parameters in the convection-dispersion model. The adsorption isotherm was fitted to the Langmuir, Freundlich, and Sips models. The Langmuir model assumes homogeneous adsorption and can be expressed as (Limousin et al. 2007; Worch 2012)

$$q_e = \frac{q_m K_L C_e}{1 + K_L C_e} \tag{10}$$

where C_e is the equilibrium concentration of the adsorbate in mg/L, q_e is the equilibrium adsorption capacity (mg/g), K_L is Langmuir constant (L/mg), and q_m (mg/g) is the maximum adsorption capacity. On the other hand, the Freundlich isotherm assumes a heterogeneous interaction between the active

Table 1 EDX analysis results for MWCNT before and after adsorption. Values represent normalized wt. %

Element	GPD (pure)	MWCNT (before adsorption	MWCNT (after adsorption
C	65.8%	97.3%	83.4%
N	11.3%	0%	9.2%
O	19.1%	2.7%	6.2%
S	3.8%	0%	1.2%

sites and the adsorbate and can be described by (Nassar 2013; Worch 2012; Yang 2003)

$$q_e = K_F C_e^{\frac{1}{n}} \tag{11}$$

where (1/g) is the Freundlich adsorption coefficient that characterizes the strength of adsorption. The exponent, n, represents the adsorption intensity which varies with the heterogeneity of the surface. The general form of the Sips model is (Foo and Hameed 2010)

$$q_e = q_m K_s C_e{}^{1/n} / \left(1 + K_s C_e{}^{1/n}\right) \tag{12}$$

where K_s (mg^{-1}) and q_{max} (mg/g) are the Sips equilibrium constant and maximum adsorption capacity, respectively. The Sips isotherm equation is characterized by the dimensionless heterogeneity factor, n, which can be used to describe the system's heterogeneity as n varies between 0 and 1 (Kumara et al. 2014). When n is unity, it implies a homogeneous adsorption process approaching a Langmuir behavior. Otherwise, it resembles a Freundlich behavior.

The experimental data obtained in this work did not follow the regular Langmuir isotherm. Rather, a strong Freundlich behavior was observed. Figure S9 shows a nonlinear fitting of q_e vs. C_e, according to Eq. 11, with an R^2 value of 0.9583, indicating a good Freundlich behavior. Also, the data were fitted to the Sips model as per Eq. 12, using nonlinear curve fitting. The fitting is shown in Fig. S10 with an R^2 value of 0.9586. The fitting parameters for the Freundlich and Sips models are tabulated in Table 2. Since the exponent n in the Sips isotherm is < 1, the adsorption of GPD can be described by Freundlich behavior. This is supported by the fitting results of Fig. S9.

The effect of solution pH

The effect of the solution's pH on the adsorption of GPD was studied in the range of 1–12. To exclude the effects of other environmental parameters, the pH study was conducted in batch mode rather than continues-flow. Figure 3a shows the effect of the solution pH on the adsorption of GPD. As pH increases, the removal efficiency of the MWCNT decreases dramatically. In acidic medium, the removal efficiency reaches 94% (at pH = 2), and it decreases to 13% at pH = 12. The behavior in Fig. 3a disagrees with the adsorption of GPD on activated carbon (Jasim et al. 2013), for mercury (II) ion adsorption on MWCNT/silica surface (Saleh 2015), and what has been observed in our previous study on the adsorption of alizarin dye on maghemite nanoparticles (Badran and Khalaf 2019).

Table 2 Fitting parameters for the batch adsorption of GPD

Freundlich			Sips			
n	K_F (mg^{-1})	R^2	n	K_S (mg^{-1})	q_m (mg/g)	R^2
1.0512	0.6083	0.9583	0.7983	0.0131	29.58	0.9586

The relationship between the solution pH and sorption capacity can be comprehended by examining the electrostatic forces within the adsorbent/adsorbate pair, as well as any acceptor–donor π interactions between the functional groups (Bakather et al. 2017; Nassar 2012; Tian et al. 2013; Worch 2012). Figure 3b illustrates the status of GPD and the MWCNT surface. The reported zero-point charge (ZPC) of native MWCNT is 5.3 (Wu and Xiong 2015; Zha et al. 2018). As a result, the adsorbent would have a net positive charge below pH 5.3 and a net negative charge above that value. Meanwhile, the reported pK_a of the GPD drug is estimated at *ca.* 8.1 (corrected from a previous value of *ca.* 5–6) (Grbic et al. 2010; Sanofi-Aventis Canada Inc. 2016). The functionality of the GPD drug is mostly due to the amino (–NH) and the sulfonyl groups (cf. Scheme 1). In acidic medium, the –NH groups are protonated forming a GPD cation (GPD^+). Beyond the pK_a of GPD, the drug remains in neutral form. Therefore, the high sorption capacity of the MWCNT in acidic medium is mostly due to the enhanced electrostatic agglomeration of the GPD adsorbed layers, and the increased solubility of GPD^+ in aqueous solution. This is supported by the Freundlich behavior mentioned earlier. As pH increases, the GPD turns neutral while the MWCNT surface becomes negatively charged, hindering the sorption capacity. In support to this mechanism, Fig. 3a shows that the GPD removal decreases significantly beyond pH 8, in full agreement with its pK_a value.

It is worth mentioning that the results of Fig. 3a are in contradiction with what was reported by Tian *et al.* for the adsorption of sulfamethoxazole and sulfapyridine, two antibiotics that contain similar functional groups to GPD, on functionalized MWCNT (Tian et al. 2013). In their work, the authors have introduced carboxyl and hydroxyl functional groups to the MWCNT surface through acid treatments. Such modification allows different types of interactions with

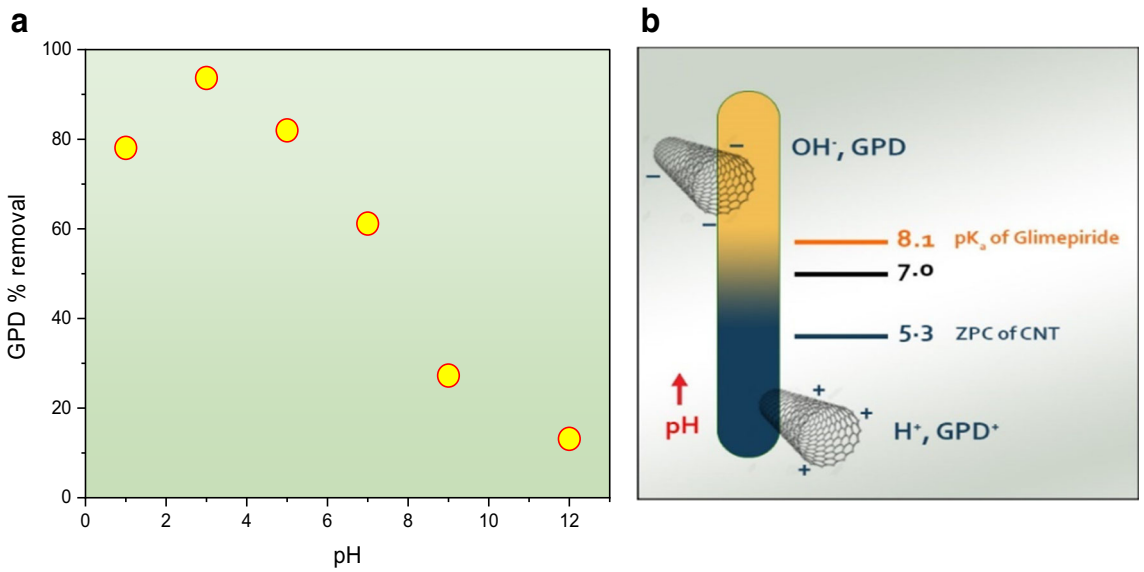

Fig. 3 **a** Effect of solution pH on the continuous adsorption of 25 ppm GPD at 25 °C. MWCNT concentration = 50 mg. **b** The GPD and MWCNT surface charges at different pH values

the adsorbate, which explains the contradictory behavior of the effect of pH.

Continuous-flow experiments

MWCNT-free trials

Prior to any experiments, the adsorption capacity of silica was evaluated by filling the fixed bed with silica only. After injecting a 25-mg/L solution of GPD, samples were taken for absorbance measurements. The results showed that there was no significant decrease in the absorbance of the sample, indicating negligible adsorption capacity of the silica.

The effect of bed height

To optimize the adsorption conditions, the effect of bed height on the removal of GPD was studied as illustrated in Fig. 4. Four different heights were examined: 1, 2, 3, and 4 cm, with each 1 cm representing 1-g silica and 40 mg of MWCNT. A constant 25:1 ratio of silica to MWCNT was used in order to isolate the effect of the adsorbent. As the figure shows, a typical S-shape of BTC is observed which is a good indication for the mass transfer and internal resistance within the column. The figure also shows that the breakthrough time is increased with increasing the bed height, due to increasing the residence time of the GPD through the bed which allows more GPD to diffuse into the adsorbent, and thus increasing the adsorption removal efficiency. This is a common phenomenon of fixed-bed adsorption because as the amount of MWCNT increases in the column bed, more active sites become available for adsorption (Hethnawi et al. 2020a; Tian et al. 2013). The removal of GPD, represented by the decrease in its absorbance, was best at 3–4 cm. Therefore, the rest of the study was completed using 3 cm.

The effect of flow rate

The effect of solution flow rate on the adsorptive removal of GPD is illustrated in Fig. 5. The figure demonstrates the enhancement of GPD removal as the flow rate decreases. At a flow rate of 2 mL/min, the break point (T_b) is almost 17 min. As the flow rate increases to 6 mL/min, the T_b decreased to almost 2 min. This result can be rationalized based on the residence time required for the GPD molecules to be adsorbed on the MWCNT surface in the mass transfer zone (MTZ) (cf. Fig. 1). As the flow rate of the GPD increases at the inlet, the residence time decreases, and less adsorption sites are

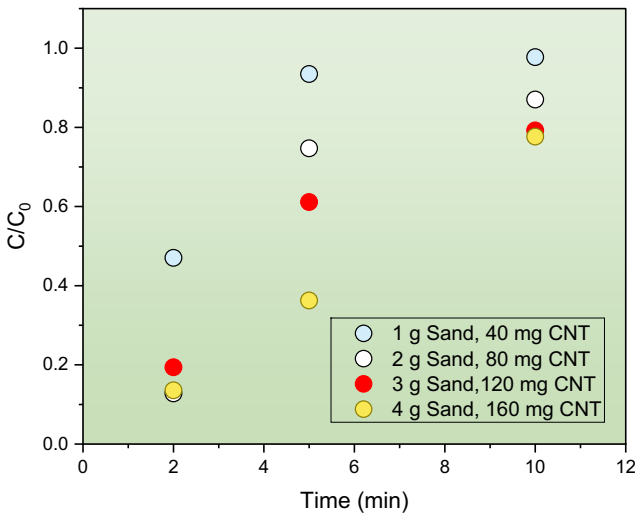

Fig. 4 Effect of bed height on the adsorption on 25-ppm GPD adsorption, using constant ratio of silica to CNT at 25 °C, and pH ≈ 7.

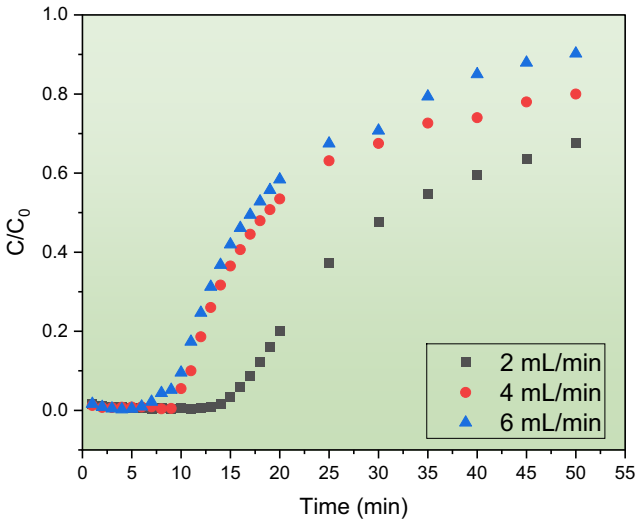

Fig. 5 Effect of flow rate on the continuous adsorption of 25 mg/L GPD at 25 °C, and pH ≈ 7, MWCNT concentration = 400 mg, bed height = 3 cm

occupied per minute. As a result, the front of the MTZ reaches the bottom of the bed column in less time causing a reduction in the removal efficiency. This result is an agreement with previous studies on the adsorption of metal ions and organic dyes on pyroxene nanoparticles (Hethnawi et al. 2020a; Hethnawi et al. 2020b; Hethnawi et al. 2017a; Tian et al. 2013).

The effect of adsorbent dosage and the breakthrough curves

The investigations of the parameters affecting the adsorption of GPD were used to study the effect of the amount of the MWCNT adsorbent. The breakthrough curves for different masses of MWCNT in the column obtained with a 25-mg/L concentration of GPD and 4.0 ml/min flow rate are shown in Fig. 6a. As shown, the obtained experimental data fit very well with the convection–dispersion model (Eq. 6), and the BTC curves have S-shape profile which is a good indication for mass transfer and internal resistance effects within the column. The accuracy in fitting was also evident from the low values of chi-square (χ^2) as displayed in Table 2. The table shows the axial dispersion coefficient (D_L) along with χ^2 for each breakthrough curves. As shown in the figure, by increasing the MWCNT amount from 100 to 400 mg (in a silica bed-height of 3 cm), the capacity of MWCNT to adsorb GPD increases which results in a delay to obtain the breakthrough time (T_b) from 1.6 to almost 14.7 min and also increase in volume of treated water. These findings were also supported by values of the axial dispersion coefficient (D_L) using the convection–dispersion model. Hence, the D_L value is decreased as concentration of MWCNT increases (from 9 to 3 × 10^{-5} m^2/s), thus confirming the delay in the break point. This finding can be explained by the high number of active/binding cites available due to the high surface area provided with high dosage of MWCNT. However, the amount of MWCNT used in the removal of GPD from aqueous solutions is crucial for the commercial application due to the cost value of MWCNT. Therefore, the amount of MWCNT must be optimized for large-scale fixed-bed column uses. Moreover, the pore structure of MWCNT may also influence the adsorption behavior of GPD. The MWCNT exhibits an open-pore network that may facilitate fast molecular diffusion and promotes the accessibility of adsorption sites. This fact was also supported by the high order of magnitude for D_L (10^{-5} m^2/s) for MWCNT which is higher than that of fixed-bed absorber using activated carbon (AC) or diatomite (Hethnawi et al. 2018). AC, for instance, usually comprises a large portion of small micropores with closed and

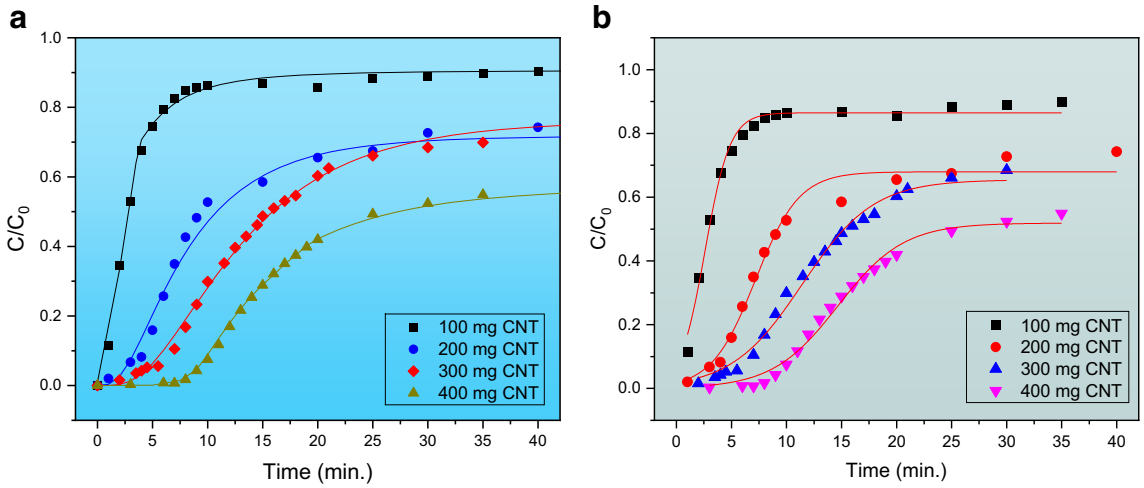

Fig. 6 **a** BTCs for adsorption of GPD onto different dosage of MWCNT over silica (100, 200, 300, and 400 mg MWCNT). The points represent the experimental data. The solid lines represent a curve fitting according to the convection–dispersion model (Eq. 6). **b** The data fitting for the Thomas model. Experimental operating conditions: C_0 = 25 mg/L, Q = 4 mL/min, Z = 3 cm, and T = 25 °C

Table 3 BTC parameters for the adsorption of GPD at different concentrations of MWCNT using the dispersion–convection and Thomas models. C_0 = 25 mg/L, bed height = 3 cm, flow rate = 4 ml/min, and 25 °C

MWCNT dosage (mg)	T_b (min)	Dispersion–convection model		Thomas model		
		$D_L \times 10^5$ (m^2/s)	χ^2	K_{TH} (mL mg^{-1} min^{-1}) × 10^{-2}	q_0 (mg/g)	R^2
400	14.7	3.5	0.42	1.34	275.3	0.9865
300	11.4	4.8	0.21	1.24	214.5	0.9901
200	6.3	7.3	0.19	2.01	134.4	0.9777
100	1.6	9.0	0.16	3.53	48.8	0.9866

irregular-shaped structure. This micropore is responsible for the provided surface area; thus, filling these micropores will significantly affect the adsorption capacity and lowering the value of the axial dispersion coefficient. Therefore, the high degree of graphitization of the MWCNT surface and the open-pore structure are the main factors for superior adsorption properties of MWCNT (Wang et al. 2014).

Furthermore, nonlinear curve fittings for the Adams–Bohart and Thomas models were also applied to the breakthrough curves as described in the experimental section. The Adams–Bohart model has failed to describe the adsorption data as shown in Fig. S11. On the other hand, the Thomas model managed to predict the adsorption breakthrough curves to a great extent as seen in Fig. 6b. The fitting parameters for the convection–dispersion and Thomas models are shown in Table 3. The maximum adsorption capacity q_0 determined by using the Thomas model (cf. Eqs. 1 and 2) ranges between 48.8 and 275.3 mg/g. The maximum value is obtained with 400 mg of MWCNT. This reflects the high adsorption capacity of the MWCNT to absorb pharmaceuticals such as GPD. Also, Fig. 6b illustrates that removal efficiency is > 95%.

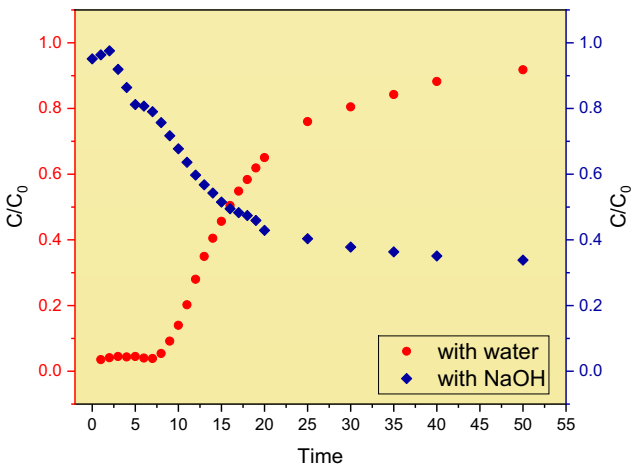

Fig. 7 Regenerating the adsorption column through flushing with NaOH and deionized water for 50 min. GPD concentration = 25 mg/L, 25 °C. pH ≈ 7, bed height = 3 cm

Adsorbent regeneration

As this study aims to construct a proof-of-concept for a full continuous-flow adsorption model for GPD from wastewater resources, an attempt to regenerate the MWCNT adsorbent was made. The results obtained from the pH study (Section 3.1.2) revealed that sorption of GPD on the MWCNT is best in acidic medium. Therefore, washing the MWCNT with an alkaline solution should regenerate the adsorbent surface. Figure 7 shows the adsorption BTC of the drug after flushing the column with 0.1 M NaOH solution (blue points) and deionized water (red points) for 10 min. The flushing was performed after a routine run using MWCNT and silica for 50 min. When the column is flushed with water, the performance of the adsorption column pertained only for 5 min before the effluent concentration starts to increase. Yet, when the column was flushed with dilute NaOH, the column stayed functional for more than 50 min. Therefore, MWCNT can be reused in the column bed repeatedly to save costs.

Conclusions

The adsorptive removal of the antidiabetic drug glimepiride (GPD) was studied in batch and continuous modes for wastewater treatment purposes. Commercial multi-walled carbon nanotubes (MWCNT) were used as adsorbent. Different dynamical parameters were investigated, including the solution pH, column height, flow rate, and amount of adsorbent. The batch experiments showed that the adsorption isotherm has followed a Freundlich behavior. The maximum adsorption capacity (q_0) was determined to be 275.3 mg/g, with > 98% removal efficiency. Based on the considerations of the zero-point charge (ZPC) of the MWCNT and the pK_a of the drug, the adsorption efficiency was enhanced significantly in acidic medium, and maximized at pH = 2. Also, the adsorption efficiency was increasing with decreasing flow rate and increasing bed height and amount of adsorbent. The continuous-flow experiments were performed using a fixed bed filled with

MWCNT dispersed in silica. A new convection–dispersion model coupled with Freundlich model, in addition to the conventional Thomas model, was used to describing the adsorption breakthrough curve. It was found that the convection-dispersion model has predicted the curve to a very good extent. The axial dispersion coefficients were ranged between 3.5 and 9.0 × 10^5 m^2/s. Finally, flushing the column bed with a dilute solution of NaOH was successful in regenerating the MWCNT adsorbent.

The outcomes of this study can be used to construct an industrial adsorber that utilizes cheap silica and small amount of MWCNT to treat polluted water from micropollutants, including GPD. The mathematical fitting of the convection-dispersion model can be also used to deduce other important parameters that are required for industrial implementation of the treatment process.

Supplementary Information The online version contains supplementary material available at https://doi.org/10.1007/s11356-020-11679-y.

Acknowledgments The authors are grateful to the Faculty of Science at An-Najah National University and the College of Arts and Sciences at Qatar University for supporting this research. The authors are thankful to the staff at the Central Lab Unit (CLU) at Qatar University for helping in performing the SEM/EDX analysis. We would like to acknowledge Carbon OxyTech Inc., Calgary, Alberta, Canada, for providing the multi-walled carbon nanotubes (MWCNT), for modeling the experimental data, and for providing their valuable feedback and materials. The authors are thankful to Dr. Amjad Shraim at Qatar University and Mr. Ismail Almanassra at Hamad Bin Khalifa University for their valuable consultations.

Authors' contributions IB led the project, designed the experiments, analyzed the data, and performed the mathematical modeling. OQ performed the experimental work and analyzed the results. AM participated in designing the experiments, analyzed the experimental data, and performed the mathematical modeling. MA provided the technical guidelines for the pharmaceuticals and participated in designing the experiments. All the authors read and approved the final manuscript.

Funding This research was funded by the Faculty of Science at An-Najah National University, Nablus, Palestine, general graduate students funding.

Data availability All the data generated or analyzed during this study are included in this published article (and its supplementary information files).

Compliance with ethical standards

Ethics approval and consent to participate Not applicable

Consent for publication Not applicable

Conflict of interest The authors declare that there is no conflict of interest.

Authors' information (optional) Authors' information is provided in the first page.

References

Abraham DJ, Tilley J, Grimsby J, Erickson S, Berthel S (2010) Diabetes drugs: present and emerging. In: Abraham DJ (ed) Burger's medicinal chemistry and drug discovery. https://doi.org/10.1002/0471266949.bmc198

Ahsan MA et al (2020) Tissue paper-derived porous carbon encapsulated transition metal nanoparticles as advanced non-precious catalysts: carbon-shell influence on the electrocatalytic behaviour. J Colloid Interface Sci 581:905–918

Ajmal A, Majeed I, Malik RN, Idriss H, Nadeem MA (2014) Principles and mechanisms of photocatalytic dye degradation on TiO2 based photocatalysts: a comparative overview. RSC Adv 4:37003–37026. https://doi.org/10.1039/C4RA06658H

Allied Market Research (2020) Carbon nanotubes (CNTs) Market Overview. http://www.alliedmarketresearch.com/press-release/carbon-nanotube-market.html

Alnajjar M, Hethnawi A, Nafie G, Hassan A, Vitale G, Nassar NN (2019) Silica-alumina composite as an effective adsorbent for the removal of metformin from water. J Environ Chem Eng 7:102994. https://doi.org/10.1016/j.jece.2019.102994

Altowayti WAH, Allozy HGA, Shahir S, Goh PS, Yunus MAM (2019) A novel nanocomposite of aminated silica nanotube (MWCNT/Si/NH2) and its potential on adsorption of nitrite. Environ Sci Pollut Res 26:28737–28748. https://doi.org/10.1007/s11356-019-06059-0

Asplund K, Wiholm BE, Lithner F (1983) Glibenclamide-associated hypoglycaemia: a report on 57 cases. Diabetologia 24:412–417. https://doi.org/10.1007/bf00257338

Badran I, Khalaf R (2019) Adsorptive removal of alizarin dye from wastewater using maghemite nanoadsorbents. Sep Sci Technol 55:2433–2448. https://doi.org/10.1080/01496395.2019.1634731

Badran I, Talie Z (2020) Kinetics of alizarin dye hydrolysis in alkaline medium for wastewater treatment Iran. J Chem Chem Eng (IJCCE). https://doi.org/10.30492/IJCCE.2020.39818

Badran I, Hassan A, Manasrah AD, Nassar NN (2019a) Experimental and theoretical studies on the thermal decomposition of metformin. J Therm Anal Calorim 138:433–441. https://doi.org/10.1007/s10973-019-08213-9

Badran I, Manasrah AD, Nassar Nashaat N (2019b) A combined experimental and density functional theory study of metformin oxy-cracking for pharmaceutical wastewater treatment. RSC Adv 9:13403–13413. https://doi.org/10.1039/C9RA01641D

Badran I, Manasrah AD, Hassan A, Nassar NN (2020) Kinetic study of the thermo-oxidative decomposition of metformin by isoconversional and theoretical methods. Thermochim Acta:178797. https://doi.org/10.1016/j.tca.2020.178797

Bakather OY, Kayvani Fard A, Ihsanullah KM, Nasser MS, Atieh MA (2017) Enhanced adsorption of selenium ions from aqueous solution using iron oxide impregnated carbon nanotubes. Bioinorg Chem Appl 2017:4323619–4323612. https://doi.org/10.1155/2017/4323619

Biel-Maeso M, Corada-Fernández C, Lara-Martín PA (2018) Monitoring the occurrence of pharmaceuticals in soils irrigated with reclaimed wastewater. Environ Pollut 235:312–321. https://doi.org/10.1016/j.envpol.2017.12.085

Bohart G, Adams E (1920) Some aspects of the behavior of charcoal with respect to chlorine. J Am Chem Soc 42:523–544

Bradley PM, Journey CA, Button DT, Carlisle DM, Clark JM, Mahler BJ, Nakagaki N, Qi SL, Waite IR, VanMetre PC (2016) Metformin and other pharmaceuticals widespread in wadeable streams of the southeastern United States. Environ Sci Technol Lett 3:243–249. https://doi.org/10.1021/acs.estlett.6b00170

Burge MR, Schmitz-Fiorentino K, Fischette C, Qualls CR, Schade DS (1998) A prospective trial of risk factors for sulfonylurea-induced

hypoglycemia in type 2 diabetes mellitus. Jama 279:137–143. https://doi.org/10.1001/jama.279.2.137

Carrales-Alvarado DH, Leyva-Ramos R, Rodríguez-Ramos I, Mendoza-Mendoza E, Moral-Rodríguez AE (2020) Adsorption capacity of different types of carbon nanotubes towards metronidazole and dimetridazole antibiotics from aqueous solutions: effect of morphology and surface chemistry. Environ Sci Pollut Res 27:17123–17137. https://doi.org/10.1007/s11356-020-08110-x

Charumathi D, Das N (2012) Packed bed column studies for the removal of synthetic dyes from textile wastewater using immobilised dead C. tropicalis. Desalination 285:22–30. https://doi.org/10.1016/j.desal.2011.09.023

Couto CF, Lange LC, Amaral MCS (2019) Occurrence, fate and removal of pharmaceutically active compounds (PhACs) in water and wastewater treatment plants—a review. J Water Process Eng 32:100927. https://doi.org/10.1016/j.jwpe.2019.100927

Dong S, Feng J, Fan M, Pi Y, Hu L, Han X, Liu M, Sun J, Sun J (2015) Recent developments in heterogeneous photocatalytic water treatment using visible light-responsive photocatalysts: a review. RSC Adv 5:14610–14630. https://doi.org/10.1039/C4RA13734E

El-sayed MEA (2020) Nanoadsorbents for water and wastewater remediation. Sci Total Environ 739:139903. https://doi.org/10.1016/j.scitotenv.2020.139903

Fent K, Weston AA, Caminada D (2006) Ecotoxicology of human pharmaceuticals. Aquat Toxicol 76:122–159

Foo KY, Hameed BH (2010) Insights into the modeling of adsorption isotherm systems. Chem Eng J 156:2–10. https://doi.org/10.1016/j.cej.2009.09.013

Gadipelly C, Pérez-González A, Yadav GD, Ortiz I, Ibáñez R, Rathod VK, Marathe KV (2014) Pharmaceutical industry wastewater: review of the technologies for water treatment and reuse. Ind Eng Chem Res 53:11571–11592

Gangji AS, Cukierman T, Gerstein HC, Goldsmith CH, Clase CM (2007) A systematic review and meta-analysis of hypoglycemia and cardiovascular events: a comparison of glyburide with other secretagogues and with insulin. Diabetes Care 30:389–394

Ghosh A, Chakrabarti S, Biswas K, Ghosh UC (2015) Column performances on fluoride removal by agglomerated Ce(IV)–Zr(IV) mixed oxide nanoparticles packed fixed-beds. J Environ Chem Eng 3:653–661. https://doi.org/10.1016/j.jece.2015.02.001

Grbic S, Parojcic J, Malenovic A, Djuric Z, Maksimovic M (2010) A contribution to the glimepiride dissociation constant determination. J Chem Eng Data 55:1368–1371. https://doi.org/10.1021/je900546z

Gribble F, Reimann F (2003) Sulphonylurea action revisited: the post-cloning era. Diabetologia 46:875–891

Hethnawi A, Nassar NN, Manasrah AD, Vitale G (2017a) Polyethylenimine-functionalized pyroxene nanoparticles embedded on diatomite for adsorptive removal of dye from textile wastewater in a fixed-bed column. Chem Eng J 320:389–404. https://doi.org/10.1016/j.cej.2017.03.057

Hethnawi A, Nassar NN, Vitale G (2017b) Preparation and characterization of polyethylenimine-functionalized pyroxene nanoparticles and its application in wastewater treatment. Colloids Surf A Physicochem Eng Asp 525:20–30. https://doi.org/10.1016/j.colsurfa.2017.04.067

Hethnawi A, Manasrah AD, Vitale G, Nassar NN (2018) Fixed-bed column studies of total organic carbon removal from industrial wastewater by use of diatomite decorated with polyethylenimine-functionalized pyroxene nanoparticles. J Colloid Interface Sci 513:28–42. https://doi.org/10.1016/j.jcis.2017.10.078

Hethnawi A, Alnajjar M, Manasrah AD, Hassan A, Vitale G, Jeong R, Nassar NN (2020a) Metformin removal from Water Using fixed-bed column of silica-alumina composite. Colloids Surf A Physicochem Eng Asp:124814. https://doi.org/10.1016/j.colsurfa.2020.124814

Hethnawi A, Khderat W, Hashlamoun K, Kanan A, Nassar NN (2020b) Enhancing chromium (VI) removal from synthetic and real tannery effluents by using diatomite-embedded nanopyroxene. Chemosphere 252:126523. https://doi.org/10.1016/j.chemosphere.2020.126523

Jasim SM, Baban RS, Jasim HS (2013) Adsorption of glimepiride on activated charcoal and Iraqi kaolin from aqueous solution Iraqi. J Med Sci 11:24–32

Kibuye FA, Gall HE, Elkin KR, Ayers B, Veith TL, Miller M, Jacob S, Hayden KR, Watson JE, Elliott HA (2019) Fate of pharmaceuticals in a spray-irrigation system: from wastewater to groundwater. Sci Total Environ 654:197–208. https://doi.org/10.1016/j.scitotenv.2018.10.442

Kiran T, Shastri N, Ramakrishna S, Sadanandam M (2009) Surface solid dispersion of glimepiride for enhancement of dissolution rate. Int J Pharmtech Res 1:822–831

Kot-Wasik A, Jakimska A, Śliwka-Kaszyńska M (2016) Occurrence and seasonal variations of 25 pharmaceutical residues in wastewater and drinking water treatment plants. Environ Monit Assess 188:661. https://doi.org/10.1007/s10661-016-5637-0

Kumara NTRN, Hamdan N, Petra MI, Tennakoon KU, Ekanayake P (2014) Equilibrium isotherm studies of adsorption of pigments extracted from Kuduk-kuduk (Melastoma malabathricum L.) pulp onto TiO2 nanoparticles. J Chem 2014. https://doi.org/10.1155/2014/468975

Li Z, Sobek A, Radke M (2016) Fate of pharmaceuticals and their transformation products in four small European rivers receiving treated wastewater. Environ Sci Technol 50:5614–5621. https://doi.org/10.1021/acs.est.5b06327

Li Z, Gómez-Avilés A, Sellaoui L, Bedia J, Bonilla-Petriciolet A, Belver C (2019) Adsorption of ibuprofen on organo-sepiolite and on zeolite/sepiolite heterostructure: synthesis, characterization and statistical physics modeling. Chem Eng J 371:868–875

Limousin G, Gaudet J-P, Charlet L, Szenknect S, Barthes V, Krimissa M (2007) Sorption isotherms: a review on physical bases, modeling and measurement. Appl Geochem 22:249–275

Liu X, O'Carroll DM, Petersen EJ, Huang Q, Anderson CL (2009) Mobility of multiwalled carbon nanotubes in porous media. Environ Sci Technol 43:8153–8158. https://doi.org/10.1021/es901340d

Luo Y, Guo W, Ngo HH, Nghiem LD, Hai FI, Zhang J, Liang S, Wang XC (2014) A review on the occurrence of micropollutants in the aquatic environment and their fate and removal during wastewater treatment. Sci Total Environ 473-474:619–641. https://doi.org/10.1016/j.scitotenv.2013.12.065

Mackuľak T, Černanský S, Fehér M, Birošová L, Gál M (2019) Pharmaceuticals, drugs, and resistant microorganisms — environmental impact on population health. Curr Opin Environ Sci Health 9:40–48. https://doi.org/10.1016/j.coesh.2019.04.002

Manasrah AD, Nassar NN (2020) Oxy-cracking technique for producing non-combustion products from residual feedstocks and cleaning up wastewater. Appl Energy 280:115890. https://doi.org/10.1016/j.apenergy.2020.115890

Manasrah AD, al-Mubaiyedh UA, Laui T, Ben-Mansour R, al-Marri MJ, Almanassra IW, Abdala A, Atieh MA (2016) Heat transfer enhancement of nanofluids using iron nanoparticles decorated carbon nanotubes. Appl Therm Eng 107:1008–1018. https://doi.org/10.1016/j.applthermaleng.2016.07.026

Manasrah AD, Almanassra Ismail W, Marei NN, Al-Mubaiyedh UA, Laoui T, Atieh MA (2018) Surface modification of carbon nanotubes with copper oxide nanoparticles for heat transfer enhancement of nanofluids. RSC Adv 8:1791–1802. https://doi.org/10.1039/C7RA10406E

Marchetti P, Navalesi R (1989) Pharmacokinetic-pharmacodynamic relationships of oral hypoglycaemic agents. An update. Clin

Pharmacokinet 16:100–128. https://doi.org/10.2165/00003088-198916020-00004

Markiewicz M, Jungnickel C, Stolte S, Białk-Bielińska A, Kumirska J, Mrozik W (2017) Primary degradation of antidiabetic drugs. J Hazard Mater 324:428–435

Mrozik W, Stefańska J (2014) Adsorption and biodegradation of antidiabetic pharmaceuticals in soils. Chemosphere 95:281–288. https://doi.org/10.1016/j.chemosphere.2013.09.012

Nassar NN (2012) Iron oxide nanoadsorbents for removal of various pollutants from wastewater: an overview. In: Application of adsorbents for water pollution control. Bentham Science Publishers, pp 81–118. https://doi.org/10.2174/97816080526911120101

Nassar NN (2013) The application of nanoparticles for wastewater remediation. In: Applications of nanomaterials for water quality. Future Medicine, London, pp 52–65. https://doi.org/10.4155/ebo.13.373

Niemuth NJ, Jordan R, Crago J, Blanksma C, Johnson R, Klaper RD (2015) Metformin exposure at environmentally relevant concentrations causes potential endocrine disruption in adult male fish. Environ Toxicol Chem 34:291–296. https://doi.org/10.1002/etc.2793

OriginLab Corporation (2020) Origin 2020: scientific data analysis and graphing software. OriginLab Corporation, Northampton

Proks P, Reimann F, Green N, Gribble F, Ashcroft F (2002) Sulfonylurea stimulation of insulin secretion. Diabetes 51:S368–S376

Saleh TA (2015) Mercury sorption by silica/carbon nanotubes and silica/activated carbon: a comparison study. J Water Supply Res Technol AQUA 64:892–903

Sanofi-Aventis Canada Inc (2016). AMARYL "Glimepiride", manufacturer's standard. AMARY "Glimepiride". Laval, Quebec, Canada. http://products.sanofi.ca/en/amaryl.pdf

Sarkar S, Das R, Choi H, Bhattacharjee C (2014) Involvement of process parameters and various modes of application of TiO2 nanoparticles in heterogeneous photocatalysis of pharmaceutical wastes – a short review. RSC Adv 4:57250–57266. https://doi.org/10.1039/C4RA09582K

Saudek CD, Derr RL, Kalyani RR (2006) Assessing glycemia in diabetes using self-monitoring blood glucose and hemoglobin A1c. Jama 295:1688–1697. https://doi.org/10.1001/jama.295.14.1688

Sylvia N, Hakim L, Fardian N, Yunardi (2018) Adsorption performance of fixed-bed column for the removal of Fe (II) in groundwater using activated carbon made from palm kernel shells. IOP Conf Ser Mater Sci Eng https://doi.org/10.1088/1757-899x/334/1/012030

Thomas HC (1944) Heterogeneous ion exchange in a flowing system. J Am Chem Soc 66:1664–1666

Tian Y, Gao B, Morales VL, Chen H, Wang Y, Li H (2013) Removal of sulfamethoxazole and sulfapyridine by carbon nanotubes in fixed-bed columns. Chemosphere 90:2597–2605. https://doi.org/10.1016/j.chemosphere.2012.11.010

Wang B, Chen W, Fu H, Qu X, Zheng S, Xu Z, Zhu D (2014) Comparison of adsorption isotherms of single-ringed compounds between carbon nanomaterials and porous carbonaceous materials over six-order-of-magnitude concentration range. Carbon 79:203–212. https://doi.org/10.1016/j.carbon.2014.07.061

Worch E (2012) Adsorption technology in water treatment. De Gruyter, Berlin, Boston https://doi.org/10.1515/9783110240238

Wu Q, Xiong Z-h (2015) Adsorption behavior of nitrofurantoin onto multi-walled carbon nanotubes and magnetite (Fe3O4)-loaded multi-walled carbon nanotubes from aqueous solution. J Dispers Sci Technol 36:821–830. https://doi.org/10.1080/01932691.2014.926251

Xu Z, J-g C, Pan B-c (2013) Mathematically modeling fixed-bed adsorption in aqueous systems. J Zhejiang Univ Sci A 14:155–176. https://doi.org/10.1631/jzus.A1300029

Yang RT (2003) Adsorbents : fundamentals and applications. Wiley-Interscience, Hoboken

Zha Y, Wang Y, Liu S, Liu S, Yang Y, Jiang H, Zhang Y, Qi L, Wang H (2018) Adsorption characteristics of organics in the effluent of ultrashort SRT wastewater treatment by single-walled, multi-walled, and graphitized multi-walled carbon nanotubes. Sci Rep 8:17245. https://doi.org/10.1038/s41598-018-35374-8

Zhu S, Liu YG, Liu SB, Zeng GM, Jiang LH, Tan XF, Zhou L, Zeng W, Li TT, Yang CP (2017) Adsorption of emerging contaminant metformin using graphene oxide. Chemosphere 179:20–28. https://doi.org/10.1016/j.chemosphere.2017.03.071